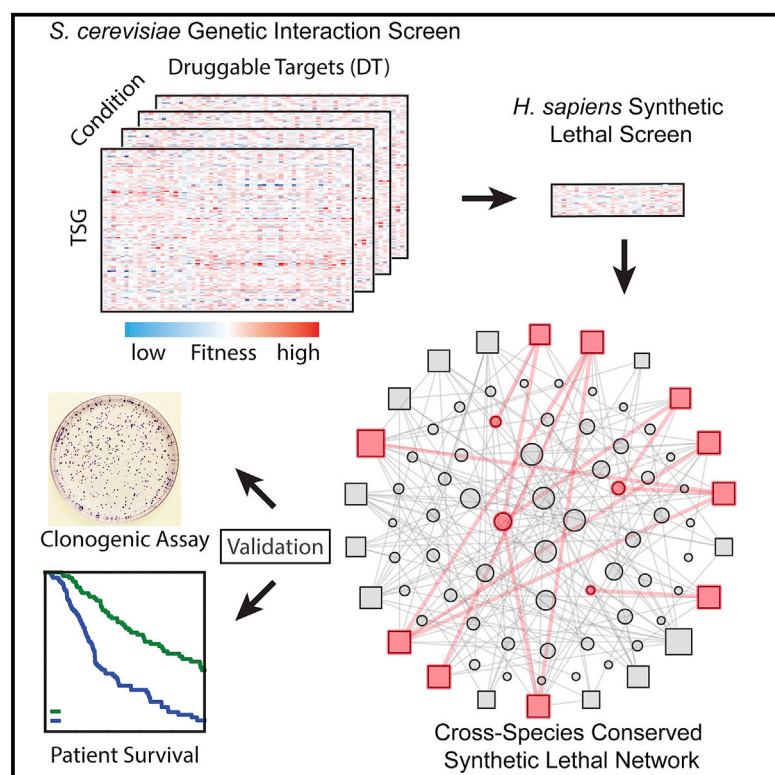# A Network of Conserved Synthetic Lethal Interactions for Exploration of Precision Cancer Therapy

Graphical Abstract

S. cerevisiae Genetic Interaction Screen

Druggable Targets (DT)

Condition

TSG

low Fitness high

Clonogenic Assay   Validation

Patient Survival

H. sapiens Synthetic Lethal Screen

Cross-Species Conserved Synthetic Lethal Network

Authors

Rohith Srivas, John Paul Shen, Chih Cheng Yang, ..., Pedro Aza-Blanc, Robert W. Sobol, Trey Ideker

Correspondence

tideker@ucsd.edu

In Brief

An emerging strategy for precision cancer therapy is to induce synthetic lethality in a tumor based on its pattern of genetic mutations. Here we map a large network of conserved synthetic lethal interactions between selective drugs and tumor suppressor genes somatically mutated in human cancer. All of these interactions are mirrored in budding yeast, an accessible model for researching drug mode of action.

Highlights

- We find a resource of conserved and divergent interactions for the design of cancer therapy

- A global yeast screen directs network assembly in human cancer cells

- As a rule, co-functionality and context stability predict translation to humans

- There are many interactions involving clinically relevant genes, including *BLM* and *XRCC3*

CrossMark

CellPress

CellPress

A Network of Conserved Synthetic Lethal Interactions for Exploration of Precision Cancer Therapy

Rohith Srivas,[1,2,9,11] John Paul Shen,[1,3,9,10] Chih Cheng Yang,[4] Su Ming Sun,[5] Jianfeng Li,[6,7] Andrew M. Gross,[8] James Jensen,[8] Katherine Licon,[1,2] Ana Bojorquez-Gomez,[2] Kristin Klepper,[1] Justin Huang,[8] Daniel Pekin,[1] Jia L. Xu,[1] Huwate Yeerna,[1] Vignesh Sivaganesh,[1] Leonie Kollenstart,[5] Haico van Attikum,[5] Pedro Aza-Blanc,[4] Robert W. Sobol,[6,7] and Trey Ideker[1,2,3,9,*]

[1]Division of Genetics, Department of Medicine, University of California San Diego, La Jolla, CA 92093, USA
[2]Department of Bioengineering, University of California San Diego, La Jolla, CA 92093, USA
[3]Moores Cancer Center, University of California San Diego, La Jolla, CA 92093, USA
[4]Functional Genomics Core, Sanford-Burnham-Prebys Medical Discovery Institute, La Jolla, CA 92037, USA
[5]Department of Human Genetics, Leiden University Medical Center, Einthovenweg 20, 2333 ZC, Leiden, the Netherlands
[6]Department of Pharmacology and Chemical Biology, University of Pittsburgh, Pittsburgh, PA 15213, USA
[7]Department of Oncologic Sciences, Mitchell Cancer Institute, University of South Alabama, Mobile, AL 36604, USA
[8]Bioinformatics and Systems Biology Program, University of California, San Diego, La Jolla, CA 92093, USA
[9]The Cancer Cell Map Initiative
[10]Co-first author
[11]Present address: Department of Genetics, Stanford University School of Medicine, Stanford, CA 94034, USA
*Correspondence: tideker@ucsd.edu
http://dx.doi.org/10.1016/j.molcel.2016.06.022

SUMMARY

An emerging therapeutic strategy for cancer is to induce selective lethality in a tumor by exploiting interactions between its driving mutations and specific drug targets. Here we use a multi-species approach to develop a resource of synthetic lethal interactions relevant to cancer therapy. First, we screen in yeast ~169,000 potential interactions among orthologs of human tumor suppressor genes (TSG) and genes encoding drug targets across multiple genotoxic environments. Guided by the strongest signal, we evaluate thousands of TSG-drug combinations in HeLa cells, resulting in networks of conserved synthetic lethal interactions. Analysis of these networks reveals that interaction stability across environments and shared gene function increase the likelihood of observing an interaction in human cancer cells. Using these rules, we prioritize ~10^5 human TSG-drug combinations for future follow-up. We validate interactions based on cell and/or patient survival, including topoisomerases with *RAD17* and checkpoint kinases with *BLM*.

INTRODUCTION

Alterations to the tumor genome fall broadly into two classes: gain-of-function mutations in growth-enhancing genes (oncogenes) and loss-of-function mutations in growth-inhibitory genes (tumor suppressor genes or TSGs). Although targeting oncogenes with chemical inhibitors or therapeutic antibodies has proven to be effective for cancer therapy (Sawyers, 2004), it is not currently feasible to restore the function of mutated or deleted TSGs in the clinical setting (Morris and Chan, 2015). Rather than targeting a TSG directly, an emerging strategy is to identify "synthetic lethal" genetic interactions between the TSG and other genes so that simultaneous disruption of both gene functions causes rapid and selective cell death (Brody, 2005). For example, cells deficient for *BRCA1* have a reduced capacity for repairing double-stranded DNA breaks and are especially vulnerable to further perturbations in DNA repair pathways (Fong et al., 2009). Olaparib, a Food and Drug Administration (FDA)-approved drug, exploits this principle by targeting a component of single-stranded DNA break repair, *PARP1*, thus causing selective cell death in $BRCA1^{-/-}$ or $BRCA2^{-/-}$ cells (Lord et al., 2015).

Recent efforts to map synthetic lethal interactions in cancer typically fall into one of several categories. First, populations of tumor genomes may be analyzed statistically to detect pairs of genes that are seldom co-mutated or co-altered in the same tumor (Jerby-Arnon et al., 2014), with one interpretation being that loss of function of both genes is synthetically lethal (Ciriello et al., 2012). This approach has the advantage of directly examining patient populations, although it is much better powered to test interactions between alterations that are very common than interactions in which one or both alterations is rare (Supplemental Experimental Procedures; Figure S1A).

Second, synthetic lethal interactions may be mapped by directed combinatorial disruptions in human cell lines. Such disruptions use pairwise small interfering RNA (siRNA) knockdowns (Roguev et al., 2013), combinations of siRNA and drug treatments (Chan and Giaccia, 2011), or the CRISPR (clustered regularly interspaced short palindromic repeats)-Cas9 system to systematically test relevant interactions in an unbiased manner (Wong et al., 2016). However, the three largest screens in human

CrossMark

cells performed to date (Bassik et al., 2013; Martins et al., 2015; Wong et al., 2016), which screened approximately 4,500, 3,600, and 2,500 interactions, respectively, fall short of the required throughput to interrogate the potential interaction space of all gene pairs involving a TSG; they also have uncharacterized off-target effects (Jackson and Linsley, 2010; Tsai et al., 2015). A hybrid of the above approaches is to screen a population of cancer cell lines against directed gene knockdowns or drugs, with the aim of identifying cell line mutations that interact with particular targets (Basu et al., 2013; Cowley et al., 2014). Such hybrid methods face the challenges already mentioned, including bias toward the most commonly mutated genes.

A complementary strategy for mapping synthetic lethal interactions in cancer is to leverage conservation with genetic interactions identified more tractably in model species (Hartwell et al., 1997). In the yeasts *S. cerevisiae* and *S. pombe*, techniques such as synthetic genetic arrays (SGAs) and Pombe Epistasis Mapper (PEM) enable genetic interactions to be measured in an unbiased manner and at a very large scale, with minimal off-target effects, because the genes are disrupted by complete and specific knockout of the open reading frame (Roguev et al., 2007; Tong and Boone, 2006). Although the model organism approach is inherently limited to testing interactions of genes that are evolutionarily conserved, numerous such interactions have been observed, especially in the core conserved pathways in which TSGs are known to operate, such as cell cycle, genome maintenance, and metabolic growth (Roguev et al., 2008; Ryan et al., 2012). A number of TSGs important for human cancer were first identified and studied in yeast (Deshpande et al., 2013; Huang et al., 2003), which also provides an accessible model system in which to study mechanism of action (Simon et al., 2000). Nonetheless, it remains unclear to what extent synthetic lethal interactions observed in a model species can be ultimately translated for clinical application. Multiple factors have been postulated to influence whether an interaction will be translatable, including the genetic, epigenetic, and environmental context (Nijman and Friend, 2013). A proper study of such factors would require a large cross-species dataset of genetic interactions relevant to cancer genes and functions.

Here we generate such a comprehensive resource of conserved synthetic lethal interactions for the study of cancer cell biology and the design of targeted therapy. This network includes quantitative tests for interaction among many TSGs in yeast and genes that are currently targetable by selective inhibitors ("druggable" targets or DTs). Strong interactions in this dataset are used to design a matched screen for lethal TSG-DT combinations in human cancer cells. This process results in a cross-species network of conserved interactions between human and yeast, allowing us to study features that best predict conservation and to extrapolate this knowledge to evaluate many potential tumor suppressor-drug interactions.

RESULTS

Selection of Conserved Tumor Suppressor and Druggable Genes

Our overall aim was to generate a broad network of synthetic lethal interactions connecting TSGs to DTs using the high-throughput capacity of yeast as a springboard into human screens. To define a set of TSGs, we compiled a list of 129 genes known or suspected to harbor loss-of-function cancer driver mutations for which there were also orthologs in yeast (Figure 1A; Tables S1 and S2; Experimental Procedures). We examined evidence that these 129 genes were clinically relevant. On average, 73% and 36% of >6,000 tumors analyzed in the Cancer Genome Atlas (TCGA) were found to contain either a somatic mutation or homozygous copy number loss, respectively, in at least one of these TSGs (Figure 1B; Supplemental Experimental Procedures). This incidence was significantly higher than that observed for the average human gene (p < 0.001 based on 1,000 random samples; Figure 1B, inset). As expected based on sequence similarity, we found that the 111 yeast orthologs of these human TSGs were enriched for functional roles similar to their human counterparts, such as maintenance of genome integrity or coordination of cell cycle arrest (Figure 1C), indicating the relevance of these genes for studying conserved oncogenic processes.

To define a set of DTs, we began with an inclusive list of human genes either known or predicted to be druggable based on features including the presence/absence of certain protein domains and the presence/absence of binding pockets in the three-dimensional structure (Russ and Lampel, 2005). Of these, we prioritized 956 genes, mapping to 433 yeast orthologs, chosen to provide broad functional representation (Figure 1A; Tables S1 and S2; Experimental Procedures). Approximately one-third of these genes were known targets of small-molecule compounds (Wishart et al., 2008), including 189 genes that were targets of a compound currently approved for use in humans by the FDA (Figure 1A).

433/3 > 189, so must be 956/3.

A TSG-DT Genetic Interaction Map in Yeast

Next we used SGA technology in the yeast *S. cerevisiae* (Tong and Boone, 2006) to systematically test for genetic interactions among all possible TSG and DT orthologs. SGA uses high-throughput robotic colony pinning on agar to create and score growth of large numbers of double gene deletion strains in parallel, here yielding tests for interaction among 43,505 gene-gene pairs. Despite the numerous previous genetic interaction studies in yeast, the majority of this space had not yet been tested (Figure 1D; Ryan et al., 2012). In addition to untreated conditions, interactions were assayed in three environmental contexts: bleomycin, which causes single- and double-stranded DNA breaks; hydroxyurea, a ribonucleotide reductase inhibitor that interferes with DNA synthesis; and hydrogen peroxide, which causes cellular oxidation damage. Across all four environments, this dataset represented ~169,000 distinct tests of gene-gene interaction. *But 43,505 * 4 = 174020, what happened?*

The resulting growth measurements were analyzed using an established computational workflow (Collins et al., 2006) to assign quantitative S scores to all interaction measurements. Positive S scores indicate an epistatic or suppressive interaction, whereas negative S scores indicate a synthetic sick or lethal relationship (Table S2). For interaction measurements that had also been made in previous studies (untreated conditions), consistency between the new and previous scores was high (r = 0.50 ± 0.1) and on par with the consistency of these

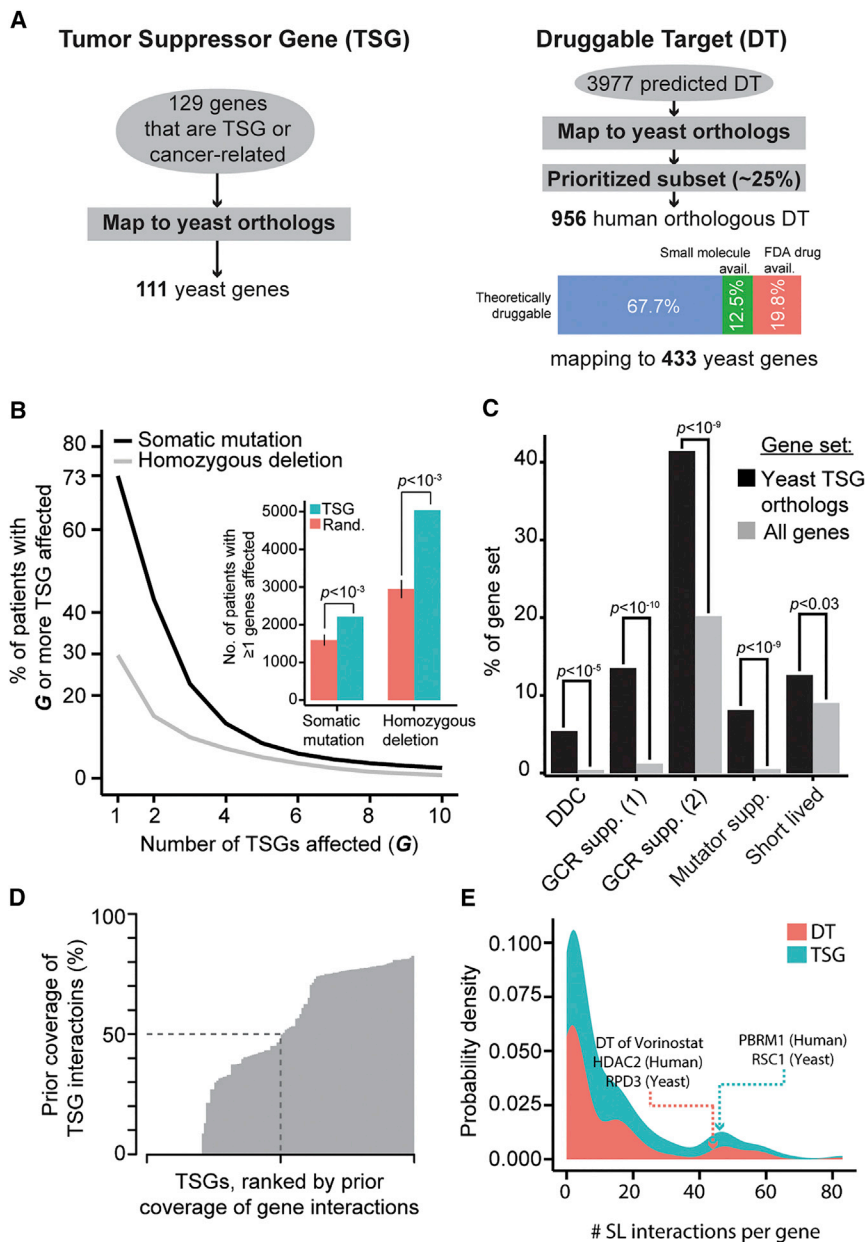## A

Tumor Suppressor Gene (TSG)

129 genes that are TSG or cancer-related

↓

Map to yeast orthologs

↓

111 yeast genes

Druggable Target (DT)

3977 predicted DT

↓

Map to yeast orthologs

↓

Prioritized subset (~25%)

↓

956 human orthologous DT

	Small molecule avail.	FDA drug avail.
Theoretically druggable		

67.7% 12.5% 19.8%

mapping to **433** yeast genes

B

C

D

E

Figure 1. Study Design and Quantitative Genetic Interaction Mapping in *S. cerevisiae*

(A) Schematic illustrating the selection of TSGs and DTs in *S. cerevisiae*.

(B) Percent of patients in TCGA harboring either a somatic mutation (n = 6,911) or homozygous deletion (n = 7,462) in any of the TSGs chosen for screening. The incidence of both somatic mutation and homozygous deletion is higher for the TSGs with yeast orthologs included in this study relative to a random set of genes (inset). The p value was calculated via 1,000 random samples. Error bars indicate ± 1 SD.

(C) Deletions of yeast TSG orthologs cause defects in cellular functions and phenotypes associated with human cancer. Significance was assessed using a Fisher's exact test. DDC, DNA damage checkpoint; taken from gene ontology (Ashburner et al., 2000). GCR Supp, gross chromosomal rearrangement suppression; lists 1 and 2 were both taken from Putnam et al. (2012). Mutator supp, mutator suppression; taken from Huang et al. (2003). Short lived, taken from Fabrizio et al. (2010).

(D) For each TSG (x axis), the plot shows the fraction of druggable genes screened for synthetic lethal interactions in prior studies in yeast (Ryan et al., 2012) (y axis). For approximately 50% of TSGs, fewer than half of the relevant interactions had been tested prior to this study (dotted lines).

(E) Number of SL hits per gene for both DTs and TSGs.

See also Figure S1 and Tables S1 and S2.

Chemo-genetic Interaction Mapping in Human Cancer Cells

Guided by the yeast network, we next performed a tumor suppressor-drug interaction screen in human cancer cells. Recognizing that no single cancer cell line can represent all of human cancer, the HeLa cervical cancer cell line was selected given its favorable cell culture characteristics and extensive molecular characterization (Adey et al., 2013). We prioritized 21 drugs for which the yeast DTs were involved in the greatest numbers of synthetic lethal interactions (interaction "hubs") (Figure 2A; Experimental Procedures). Dose-response curves of each drug were established so that the proper inhibitory concentrations could be determined (inhibitory concentration [IC]$_{20}$ and IC$_{40}$; Figure 2B; Table S3A). Yeast synthetic sick/lethal interactions with these DTs had implicated a total of 82 TSGs. To this number we added another 30 human TSGs commonly mutated in human cancers but without orthologous yeast genes.

Within this 21 drug × 112 TSG matrix (Table S3B), each drug was screened at both IC$_{20}$ and IC$_{40}$ doses in combination with each TSG knockdown. We observed minimal batch effects and high reproducibility with an average coefficient of variance (CV) of 3.8% per plate and 92% of plates having CV < 5.0% (Figure S2A). Average replicate correlation across the entire screen
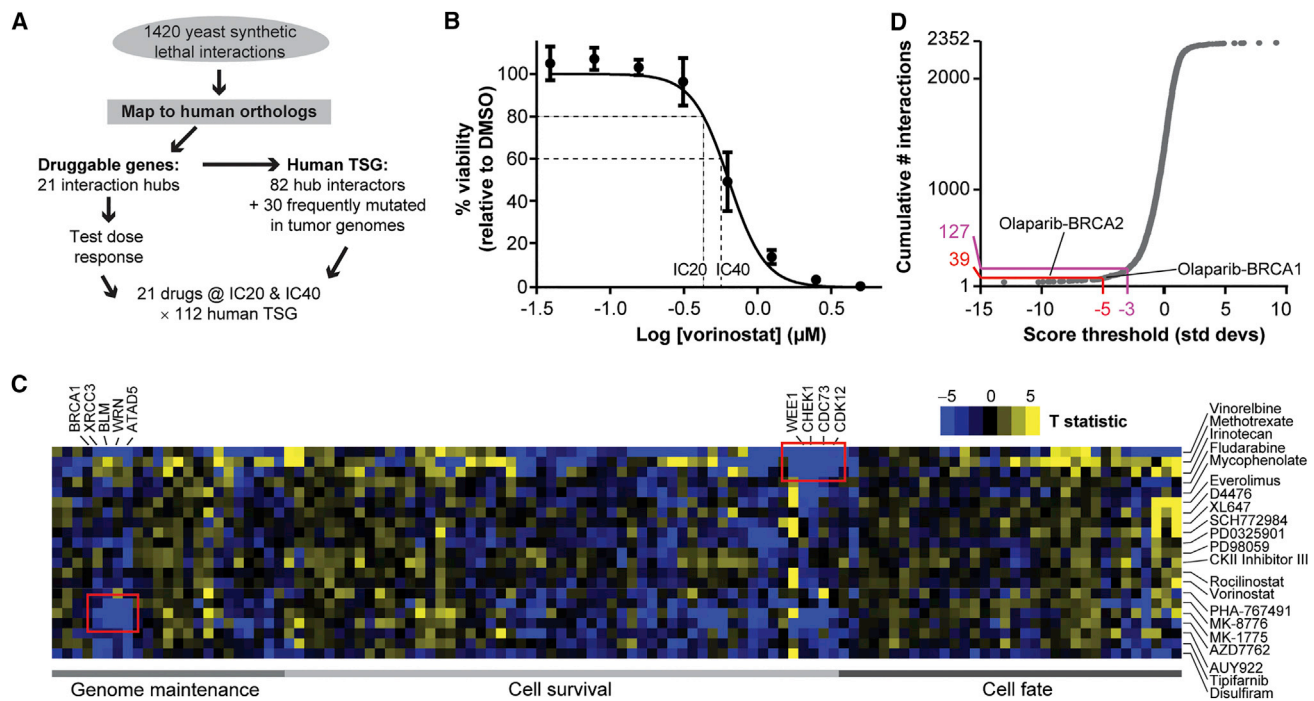
studies in comparison with one another (r = 0.58 ± 0.2) (Bandyopadhyay et al., 2010; Collins et al., 2007; Costanzo et al., 2010; Fiedler et al., 2009; Guénolé et al., 2013; Srivas et al., 2013; Wilmes et al., 2008). In total 1,420 synthetic sick/lethal interactions (S ≤ −2.5) and 996 epistatic interactions (S ≥ 2.0) were identified under untreated conditions, with an average of 14 and 11 synthetic lethal/sick interactions per TSG and DT, respectively (Figure 1E). In addition, a pan-cancer analysis of The Cancer Genome Atlas (Cancer Genome Atlas Research Network et al., 2013) identified 16 TSGs that, when mutated in tumors, are associated with coordinate upregulation in genes (false discovery rate [FDR] < 0.1) for which a negative TSG-gene interaction is found in yeast (Figures S1B and S1C; Supplemental Experimental Procedures).

Figure 2. Chemo-genetic Interaction Mapping in a Human Cancer Cell Line

(A) Design of the human screen based on the yeast network.

(B) Representative dose-response curve for the drug vorinostat. Such a curve was created for each drug to establish IC_{20} and IC_{40} doses for screening. Error bars represent ± SD.

(C) Heatmap of chemical-gene interactions. Blue represents synthetic sick/lethal (negative) interaction, and yellow represents epistatic (positive) interaction. Interactions highlighted in red are discussed in greater detail in the text.

(D) Cumulative number of interactions identified as a function of the interaction score threshold, highlighting numbers of interactions at 3 and 5 SDs (z) below the mean. Recovery of gold-standard interactions of olaparib with BRCA1 and BRCA2 is also shown.

See also Figures S2 and S4 and Tables S3 and S4.

was 0.95, which we found meets or exceeds the quality of previous genetic interaction screens in human cell lines (Figure S2B). IC_{20} and IC_{40} measurements were also significantly correlated (Figure S2C). To score chemical-gene interactions, the viability of each gene knockdown in the presence of drug was compared to the viability of non-targeting siRNA also in the presence of drug (Figure 2C; Experimental Procedures).

Applying a standard threshold of 3 SDs below the mean ($z < -3$) (Birmingham et al., 2009), a total of 127 synthetic sick/lethal genetic interactions were identified (Figure 2D; Table S4). This threshold identified the well characterized interactions of the poly ADP ribose polymerase (PARP) inhibitor olaparib with both BRCA1 and BRCA2 (Lord et al., 2015; Figure S2D). In contrast, 10-fold fewer epistatic/positive interactions were found (12 at $z > 3$), consistent with the design of the human test space based on yeast synthetic lethal interactions. Examining the entire interaction score profile of each drug, we found that drugs targeting similar proteins had similar profiles (e.g., the histone deacetylase [HDAC] inhibitors vorinostat and rocilinostat; Figure S2E).

A Conserved Synthetic Lethal Interaction Network

Having generated network resources in both yeast and human cancer cells, we were immediately interested in evidence of conservation between the two species. First, we found that gene pairs determined to interact negatively in humans had corresponding scores in yeast that were significantly more negative than the yeast scores for all remaining gene pairs. This result held true across a range of stringent cutoffs used to call human interactions but not more lenient ones (all p values are shown in Table S5A and the Supplemental Experimental Procedures). We also computed a likelihood score (LS) of human synthetic sickness/lethality provided the interaction had been first observed in yeast (Supplemental Experimental Procedures). Prior observation in yeast (i.e., gene pairs among the top 10% ranked by S score) increased the likelihood of human genetic interaction by approximately 3-fold (p < 0.031; Figure 3A; Table S5A). We note that this is less conservation than observed previously in a smaller-scale synthetic lethal screen centered around the gene FEN1 (van Pel et al., 2013).

Based on this general conservation, we next sought to identify the specific interactions with evidence of synthetic lethality in both species. To this end, we defined two conserved cancer networks (CoCaNets) of synthetic sick/lethal interactions at both lenient (10%) and stringent (2%) cutoffs: CoCaNet10 (172 interactions, top 10% based on the rank product of human and yeast scores; Supplemental Experimental Procedures) and the more stringent CoCaNet2 (36 interactions, top 2%; Figure 3B; Table
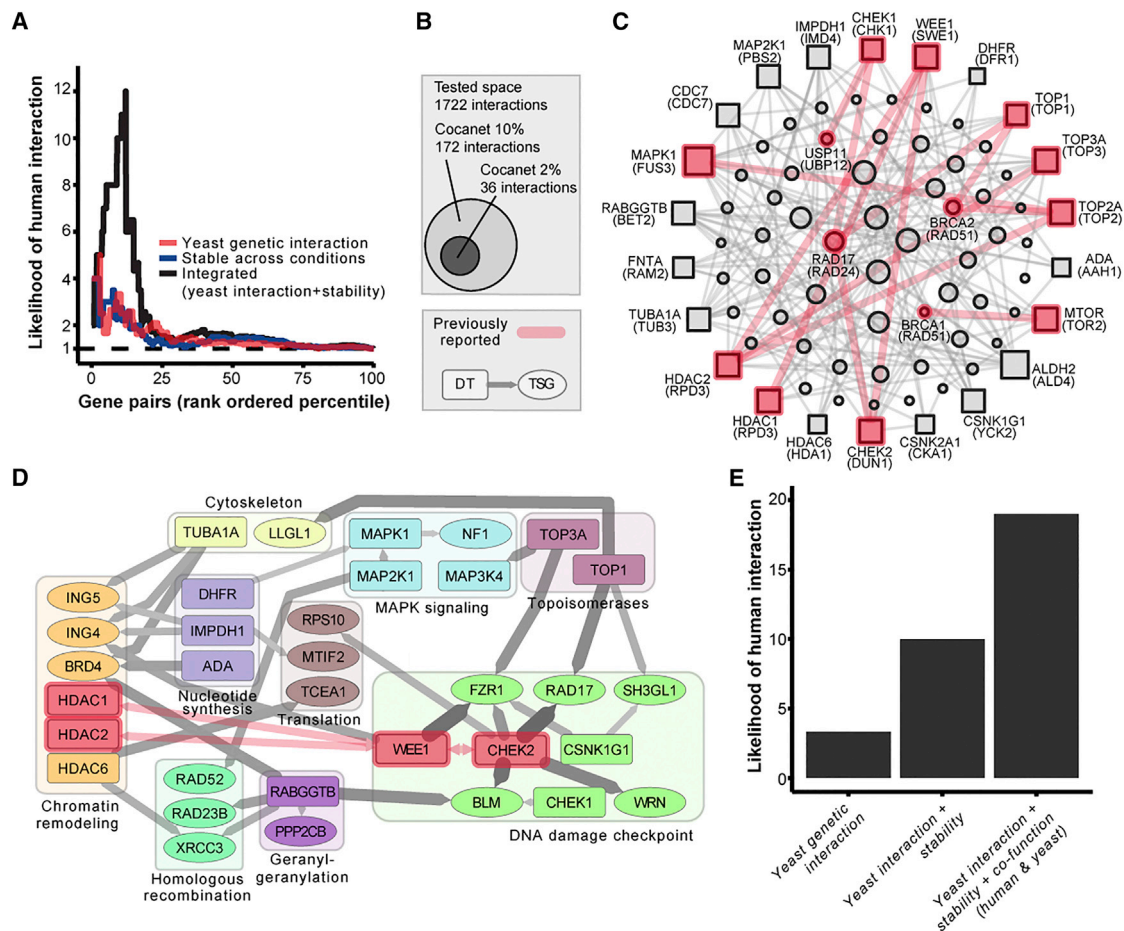
Figure 3. Conservation between Human and Yeast

(A) Evidence of synthetic lethality in yeast, as well as context stability, increases the likelihood of observing a human synthetic sick/lethal interaction. Gene pairs are ranked (x axis) by each type of evidence (colored curves). The likelihood score (y axis) is computed using synthetic lethal gene pairs identified in the human chemo-genetic screen as a gold standard (Supplemental Experimental Procedures).

(B) Venn diagram showing the number of interactions in CoCaNet (at two stringencies) relative to the number of interactions tested in both species.

(C) Network diagram of the top 10% strongest synthetic sick/lethal interactions (CoCaNet10). Square nodes on the outside ring represent DTs, and circular nodes represent TSGs. *S. cerevisiae* gene names are below human gene names in parentheses. Red edges represent interactions reported previously in the literature, and gray edges are first reported in this study.

(D) Network diagram of the top 2% strongest synthetic sick/lethal interactions (CoCaNet2) organized by gene function. The thickness of the edge represents the strength of the interaction conservation score. Arrows indicate the direction of the edge (DT to TSG).

(E) Likelihood score (for the top 10% of yeast gene pairs) for various lines of evidence.

See also Table S5.

S5B). CoCaNet10 included conserved interactions among 59 TSGs and 23 drug targets (Figure 3C). The more stringent CoCaNet2 captured the strongest conserved interactions, including those among DNA damage checkpoint, cell cycle checkpoint, topoisomerase, and chromatin remodeling genes (Figure 3D). Inspection of these networks revealed 13 interactions that had been characterized previously in humans and one in yeast, including synthetic sick relationships between *CHEK1* or *CHEK2* and *WEE1* (Carrassa et al., 2012; Chilà et al., 2015), which we recovered in both orientations (CHEK1/2 inhibitor with *WEE1* knockdown and WEE1 inhibitor with *CHEK1/2* knockdown). All remaining conserved interactions, representing the vast majority, were observed for the first time in either spe-

cies (Figures 3C and 3D). The conserved networks, along with the complete human and yeast interaction data, are available in Tables S2, S4, and S5B and have also been made available on the Network Data Exchange (NDEx, http://www.ndexbio.org; Supplemental Experimental Procedures), a database and online community for sharing and collaborative development of network models we recently launched as part of the Cytoscape Cyberinfrastructure (Pratt et al., 2015).

Incidence of Human Interaction Is Informed by Context Stability and Co-function

We next investigated whether certain network features, or rules of thumb, could increase the likelihood of observing an

interaction in HeLa cells. To this end, we annotated human gene pairs with a variety of data, including not only whether we had observed the interaction in yeast but the number of experimental contexts in which the interaction was observed (interaction stability Supplemental Experimental Procedures) and whether the genes are known to co-function in the same gene ontology (GO) biological process in either species.

Knowledge that the interaction not only occurs in yeast but is stable across environmental contexts led to an increase in the likelihood of human interaction up to 9-fold from baseline (Figure 3A). On top of this information, knowledge that a gene pair functions in the same biological process (yeast and human GO terms) increased the likelihood of human interaction to 19-fold (Figure 3E). As a negative control, we found that random permutation of features led to significantly decreased predictive capability (Table S5A; Supplemental Experimental Procedures).

Using the integrated LS score from all informative features (yeast interaction, context stability, yeast co-function, and human co-function), we then extrapolated the likelihoods of interaction to as many human gene pairs as possible, including those that were outside of our chemo-genetic screen. For this purpose, we used data from the chemo-genetic screen to train a regression model against all four features (Supplemental Experimental Procedures). In total, we assigned LSs to >100,000 human gene pairs for which all feature types were available, creating an extended CoCaNet (CoCaNetX; Table S6). CoCaNetX provides an extended set of prioritized human interactions including nearly all human TSGs and DTs for which cross-species data can be drawn by orthology to yeast. We anticipate that it will be useful for identifying potential synthetic lethal interactions in a human gene space orders of magnitude larger than that what can be experimentally tested with current technology.

Validation of Novel Interactions in Cell Survival Assays

A systematic resource of tumor suppressor interactions motivates many future studies of the feasibility of repurposing an already approved drug for selective killing of tumor cells based on specific genetic alterations. We first explored this principle in cultured tumor cells using the CoCaNet interaction neighborhoods of *RAD17* and *XRCC3*, two tumor suppressor genes involved in the repair of DNA damage. *RAD17* has a homozygous deletion in approximately 5% of prostate and ovarian cancers and mutations in approximately 5% of pancreas and stomach cancers, with sporadic alterations observed in tumors of other types. *XRCC3* is deleted in approximately 4% of bladder and pancreatic cancers (Cerami et al., 2012).

CoCaNet10 identified that *RAD17* was involved in five conserved synthetic sick/lethal interactions with topoisomerases *TOP1* and *TOP2A*, checkpoint kinases *CHEK1* and *2*, and *CSNK1G1*, the gamma isoform of casein kinase I (Figure 4A). Of these interactors, TOP1 and TOP2A are targeted by FDA-approved drugs, whereas CHEK1 and 2 are targeted by molecules in clinical development (Ashour et al., 2015; Thompson and Eastman, 2013). *CSNK1G1* is known to play a role in tumorigenesis, but its specific inhibitors have not yet entered clinical trials (Schittek and Sinnberg, 2014). Investigations in yeast had previously identified one of these interactions between the orthologs of *RAD17* and *TOP1* (Vance and Wilson, 2002), but this

interaction was identified in humans for the first time. We therefore examined the combination of chemical inhibitors targeting each of the five *RAD17* interactors with *RAD17* knockdown in clonogenic assays to ascertain whether the reduction in cell growth observed in the chemo-genetic screen, a cell population measurement, translates to a reduction in survival of individual tumor cell clones. We indeed observed that topoisomerase inhibition with irinotecan (anti-TOP1) or etoposide (anti-TOP2A) as well as casein kinase I inhibition with D4476 (anti-CSNK1G1) resulted in significantly reduced colony formation in the setting of *RAD17* knockdown relative to non-targeting control (Figures 4B–4D; Figure S3A). We also observed severe detrimental effects on colony formation when combining *RAD17* knockdown with AZD7762, a dual inhibitor of CHEK1 and 2; this interaction is explored in more detail by Shen et al. (2015).

Turning attention to the tumor suppressor *XRCC3*, CoCaNet10 showed involvement of this gene in seven conserved synthetic sick/lethal interactions (Figure 4E). Each of these interactions was interrogated by clonogenic assays of the relevant drug in combination with *XRCC3* knockdown. To determine whether the CoCaNet interactions would generalize to human cell lines other than HeLa, for the *XRCC3* neighborhood we elected to examine whether the interactions could be recovered in a different cellular background, the LN428 glioblastoma cell line (Tang et al., 2011). Five of the seven combinations were found to be associated with a negative effect on LN428 survival in a clonogenic assay, including interactions of *XRCC3* with mycophenolate mofetil (MMF, anti-IMPDH1) and vorinostat (a pan-HDAC inhibitor), both of which are FDA-approved, as well as tipifarnib (anti-RABGGTB), rocilinostat (anti-HDAC6), and entinostat (anti-HDAC1 and 2), which are in clinical development (Figures 4F and 4G; Figures S3B and S3C). The remaining two combinations, PD0325901 (anti-MAP2K1) and disulfiram (anti-ALDH2), showed no detectable survival effects. Additionally, the synthetic lethal interaction between the yeast orthologs *RPD3* and *RAD57* was confirmed in both a synthetic growth array and spot dilution assays in yeast (Figure 4H; Figure S3D). Together, these studies show that, of 12 interactions examined in a follow-up clonogenic assay, 10 could be readily associated with a specific decrease in tumor cell clonal survival, spanning two cell line backgrounds.

Implications for Clinical Translation of Synthetic Lethal Interactions

To gauge the clinical relevance of CoCaNet, we explored the association of these interactions with differences in clinical outcomes of cancer patients. Although co-mutation of both genes of a synthetic lethal pair is too rare of an event to power survival analysis, it has been shown that patients with tumors for which both genes of a synthetic sick interaction are under-expressed tend toward longer survival times (Jerby-Arnon et al., 2014). This finding is consistent with the idea that decreased function of both genes promotes synthetic sickness, causing the tumor to be less robust and leading to improved patient outcomes.

We explored evidence for this principle in the CoCaNet resource using the Jerby-Arnon et al. (2014) scoring method. Each of ~2,000 breast cancer patients profiled in the Molecular Taxonomy of Breast Cancer International Consortium (METABRIC) database (Curtis et al., 2012) was scored by
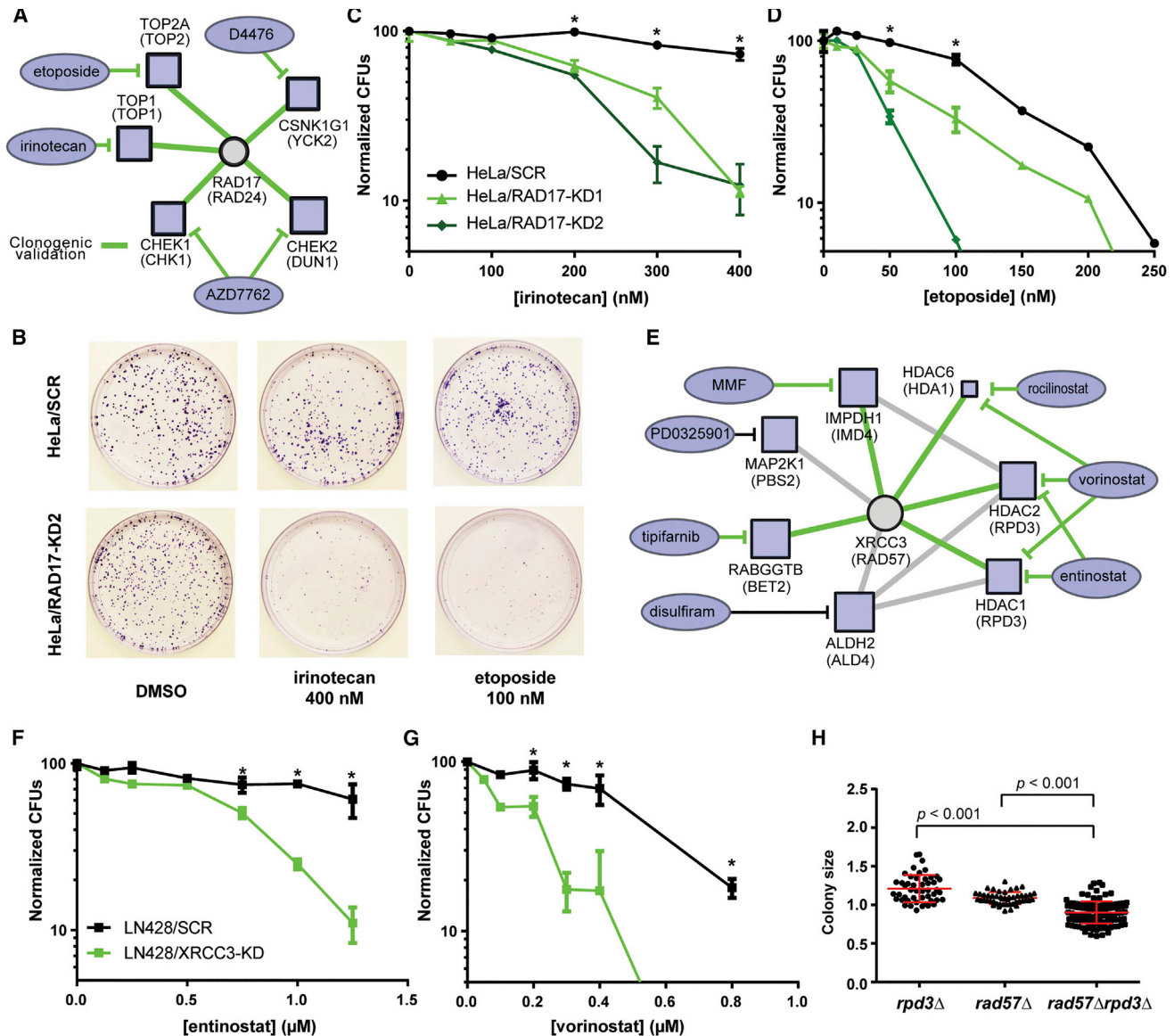
Figure 4. Validation of Cross-Species Interaction Networks for *RAD17* and *XRCC3*

(A) Network map of all conserved synthetic sick/lethal interactions in CoCaNet10 for the TSG *RAD17*. Square nodes represent druggable genes, and oval nodes represent drugs used to inhibit these genes. Green edges indicate validation by clonogenic assay.

(B) Sample plate images from the clonogenic assay.

(C) Clonogenic assay with TOP1 inhibitor irinotecan in HeLa cells with either stable knockdown of *RAD17* or non-targeting (scramble [SCR]) control. Error bars represent ± SD.

(D) Similar clonogenic assay with the TOP2 inhibitor etoposide in HeLa cells.

(E) Network map of all conserved synthetic sick/lethal interactions in CoCaNet10 for the TSG *XRCC3* with annotations as in (A).

(F) Clonogenic assay with the HDAC inhibitor entinostat in LN428 cells with either stable knockdown of *XRCC3* or non-targeting (SCR) control.

(G) Similar clonogenic assay with the HDAC inhibitor vorinostat in LN428 cells.

(H) Synthetic genetic array in *S. cerevisiae* for *rpd3Δ*, *rad57Δ*, and *rpd3Δrad57Δ*. p Values are indicated.

In (D), (F), and (G), *p < 0.05 (t test) at that dose. See also Figure S3.

counting the number of synthetic sick/lethal interactions in Co-CaNet10 for which both genes were under-expressed in the patient's tumor versus their normal tissue. The 10% of cases with the highest scores were marked as having potential "induced synthetic lethality" (ISL). The survival curve of these ISL cases

was then compared to the 10% of patients with the lowest scores (non-ISL patients).

Indeed, we found that ISL patients had significantly longer survival times relative to non-ISL patients (Figure 5A; p = 6 × 10^{-4}). Median survival had not yet been reached in this cohort;
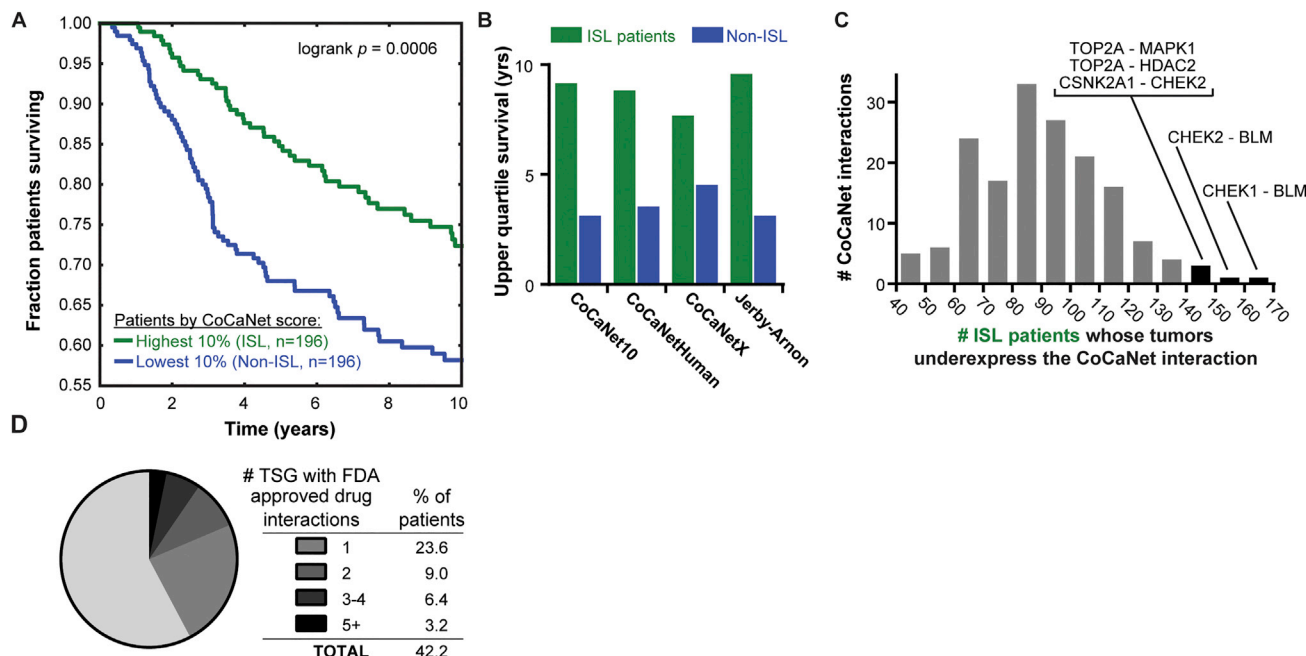
Figure 5. Clinical Potential of Deeply Conserved Interactions

(A) Kaplan-Meier plot of overall survival, selecting the highest 10% (ISL) or lowest 10% (non-ISL) of patients in METABRIC ranked by CoCaNet score.

(B) Upper-quartile survival for METABRIC cohort stratified by the indicated genetic interaction networks.

(C) Histogram of CoCaNet interactions binned by the number of patients in the ISL group in (A) whose tumors under-express both of the genes involved in the interaction.

(D) For those TSGs interacting with the target of an FDA-approved drug, the number of mutations or deletions seen per patient in the TCGA cohort.

See also Table S6.

however, the upper-quartile survival time for ISL patients was 6 years greater (9.1 years versus 3.1 years; Figure 5B). The greatest contribution to increased survival was from SL interaction of *BLM* and *CHEK1*, which were under-expressed in 162 of 196 ISL cases, followed by *BLM* and *CHEK2* (Figure 5C; Table S5B lists the contribution to patient survival of all CoCaNet interactions). Survival stratification similar to CoCaNet10 was observed when defining ISL patients purely by human chemo-genetic interactions independent of evolutionary conservation (CoCaNetHuman) and with the extended network predicted from the integrated LS score (CoCaNetX). These survival differences were also similar to those that had been observed by the original developers of this scoring approach for a different set of computationally derived synthetic lethal interactions (Jerby-Arnon et al., 2014; Figure 5B). Thus, the synthetic sick/lethal interactions in CoCaNet appear relevant to the clinical response of human tumors by this type of survival analysis.

DISCUSSION

Synthetic lethality has been of increasing interest as a strategy for cancer therapy, supported by major research investment and recent clinical success (Lord et al., 2015). Here we have realized an original proposal of Hartwell et al. (1997) in which comprehensive synthetic lethal interaction maps in yeast serve as a central resource for identifying therapeutic combinations of gene mutations and drugs in humans. Although this proposal

was advanced nearly 20 years ago, the majority of the relevant tumor suppressor interactions in either yeast or humans are being made available here for the first time. In particular, five network maps are included as part of the resource: the complete network of genetic interactions between TSGs and DTs in yeast (Table S2), the corresponding orthologous network of chemo-genetic interactions in humans (CoCaNetHuman; Figure 2; Table S4), the intersection of these datasets to derive networks of conserved interactions at two stringencies (CoCaNet2, CoCaNet10; Figure 3; Table S5B), and an extended network of predicted interactions among all human TSGs and DTs based on rules learned from study of the first four networks (CoCaNetX; Table S6).

Armed with a systematic map of tumor suppressor-drug interactions, one can begin to functionally interpret the catalog of mutations identified in cancer genome sequencing studies and to suggest therapies that might be repurposed against mutations identified in a new patient. For instance, the inhibitor of type I topoisomerases irinotecan is currently only indicated by the FDA for use in colon cancer. The conserved network resource developed here suggests that topoisomerase inhibitors should be evaluated for efficacy in cancers harboring loss-of-function alterations in *RAD17* (Figures 3C and 4A). Similarly, HDAC inhibitors such as vorinostat are currently approved for the treatment of cutaneous T cell lymphoma. Our results suggest that these drugs should also be evaluated for efficacy against tumors with *XRCC3* loss of function (Figures 3D and 4E). As clinical genomic sequencing

becomes more common, the synthetic-lethal maps provided by CoCaNetHuman, CoCaNet2/10, and CoCaNetX may become increasingly valuable tools to understand exceptional responses to therapy (Al-Ahmadie et al., 2014). In addition, these networks can continue to be curated as they are used to guide further in vitro and in vivo investigation and, ultimately, by molecular tumor boards to help identify targeted therapy for individual cancer patients (Schwaederle et al., 2014). Communal sharing, revision, and evolution of networks is a key feature of the NDEx database in which these networks are deposited (Pratt et al., 2015). The potential effect of CoCaNet on precision cancer therapy is large because more than 40% of TCGA patients have loss of function in at least one TSG with a synthetic lethal interaction involving the target of a currently FDA-approved drug (Supplemental Experimental Procedures; Figure 5D).

A specific example of how CoCaNet might be used to derive clinically actionable information involves a synthetic-sick/lethal interaction identified between irinotecan and *ATM*. In metastatic colorectal cancer (mCRC), treatment with either FOLFIRI (5-flourouracil plus irinotecan) or FOLFOX (5-flourouracil plus oxaliplatin) is indicated, with a response rate to either regimen of approximately 40%. However, diagnostic tests to determine which regimen will be most likely to induce a response for an individual patient are lacking (Choueiri et al., 2015). Because irinotecan is synthetic sick/lethal with *ATM*, FOLFIRI may be the preferred regimen in the 7% of mCRC tumors for which *ATM* has an inactivating mutation (Cancer Genome Atlas Network, 2012). Examination of TCGA mCRC cohort identifies 16 *ATM*-mutated patients, of which 6 were initially treated with irinotecan. In these patients, there is indeed a 15-month trend toward better survival (44 months versus 29 months for other regimens). Given the small sample size, this trend is not presently significant (log-rank p = 0.3), but it does prompt a follow-up study of *ATM* as a marker for irinotecan therapy.

Other examples of potential clinical translation are found in the genetic interaction profiles of three of the traditional cytotoxic chemotherapeutic drugs—vinorelbine, methotrexate, and irinotecan. Although each of these drugs has a distinct mechanism of action, all have strong interactions with multiple cancer genes involved in cell cycle regulation (*CDK12*, *CDC73*, *CHEK1*, and *WEE1*) (Figure 2C; Figure S4A). Yet another interaction cluster of interest combines commonly mutated genes in DNA damage response pathways (*BRCA1*, *XRCC3*, *BLM*, *WRN*, and *ATAD5*) with multiple chemical inhibitors of the checkpoint kinases (MK-8776, MK-1775, and AZD7762) (Figure 2C; Figure S4B). Of note, interactions with Bloom syndrome protein (*BLM*) and the checkpoint kinases *CHEK1* and *CHEK2* were the strongest contributors to the survival stratification seen in the METABRIC cohort (Figure 5C). Both CHEK1 and CHEK2 can phosphorylate *BLM*, a RecQ family DNA helicase that participates in homologous recombination, telomere maintenance, and DNA replication (Kaur et al., 2010). Such results are consistent with prior reports of synthetic lethal interactions between checkpoint kinase inhibitors and other DNA repair genes, including *TP53*, *CDKN1A*, and *RAD17* and multiple members of the Fanconi anemia pathway, as well as the fact that checkpoint kinase inhibitors synergize with radiation (Chen et al., 2009; Origanti et al., 2013;

Shen et al., 2015). The interaction cluster observed here suggests the existence of a large synthetic lethal network connecting DNA repair to cell cycle checkpoints. Given that loss-of-function events in any individual gene are typically rare in cancer (Hofree et al., 2013), the ability to identify clusters of interactions among related TSGs and drugs could allow for aggregating individual "N-of-1" patients (Collette and Tombal, 2015) into larger cohorts for more robust clinical investigation of these combinations.

As genetic interaction maps are further developed and refined in studies of human cancer, a worthy question concerns the continued value of prior screening in model organisms like yeast. Our analysis highlights several ways in which cross-species data may continue to be quite valuable. First, rapid screens in model organisms allow for very large interaction test spaces and multi-condition designs in preparation for more challenging interaction screens in humans. In this regard, screening the complete space of human TSG-DT genetic interactions is likely to remain inaccessible for some time and certainly with the precision enabled by model organism genetics. Second, an interaction conserved in yeast anchors the new finding to an experimentally tractable organism in which follow-up studies of mechanism of action may be more readily pursued. Finally, conservation in multiple species, especially those as evolutionarily divergent as yeast and humans, suggests that these interactions involve core elements of the eukaryotic cell. Might this mean that these cross-species-conserved interactions will also be relevant across a wide range of cancer cells with diverse cell lineages and genetic alterations? Although this possibility deserves further study, one might take comfort in synthetic-lethal interactions that not only relate to human cells but to creatures evolutionary divergent by more than a billion years (Nei et al., 2001).

EXPERIMENTAL PROCEDURES

Generating the Yeast Genetic Interaction Data

We constructed all possible mutants between yeast orthologs (Table S1B) of the query and array genes listed in Table S1A using SGA technology (Tong and Boone, 2006). In the final step, double mutants were pinned on agar plates containing no drugs (untreated), hydroxyurea (100 μM), bleomycin (5 μg/ml), or hydrogen peroxide (0.01%) and incubated at 30°C for either 48 hr (untreated) or 72 hr (hydroxyurea, bleomycin, and hydrogen peroxide). Pictures of the plates were taken with a Canon charge-coupled device (CCD) camera, and colony sizes were quantified using HT Colony Grid Analyzer. Finally, data were normalized, and S scores were computed using the epistatic miniarray profile (E-MAP) toolbox (Collins et al., 2006). All data are provided in Table S2. Note that data are provided for 79,184 gene pairs. These include additional data from queries/arrays screened that had no human ortholog but were included for quality control purposes.

Generating the Human Chemo-genetic Interaction Map

Starting with the DT with the greatest number of synthetic lethal interactions, we used the Drug Gene Interaction database (Griffith et al., 2013) to identify a chemical inhibitor for the first 21 of these genes. When multiple compounds were available per DT, priority was given to drugs currently approved by the FDA.

For the chemo-genetic screen, 500 cells were dispensed per well in 384-well plates and reverse-transfected with siRNAs at a final concentration of 10 nM using Lipofectamine RNAimax (Life Technologies). The 21 drugs were split into four batches. For each batch, two plates containing only DMSO solvent

were included so that the toxicity of siRNAs alone could be evaluated. Each TSG was targeted by four different siRNAs (On-Target-Plus Human Genome Collection, Dharmacon) pooled in the same well. Three independent replicates for each TSG were screened on separate assay plates at both IC_{20} and IC_{40} doses.

REFERENCES

Adey, A., Burton, J.N., Kitzman, J.O., Hiatt, J.B., Lewis, A.P., Martin, B.K., Qiu, R., Lee, C., and Shendure, J. (2013). The haplotype-resolved genome and epigenome of the aneuploid HeLa cancer cell line. Nature 500, 207–211.

Al-Ahmadie, H., Iyer, G., Hohl, M., Asthana, S., Inagaki, A., Schultz, N., Hanrahan, A.J., Scott, S.N., Brannon, A.R., McDermott, G.C., et al. (2014). Synthetic lethality in ATM-deficient RAD50-mutant tumors underlies outlier response to cancer therapy. Cancer Discov. 4, 1014–1021.

Ashburner, M., Ball, C.A., Blake, J.A., Botstein, D., Butler, H., Cherry, J.M., Davis, A.P., Dolinski, K., Dwight, S.S., Eppig, J.T., et al.; The Gene Ontology Consortium (2000). Gene ontology: tool for the unification of biology. Nat. Genet. 25, 25–29.

Ashour, M.E., Atteya, R., and El-Khamisy, S.F. (2015). Topoisomerase-mediated chromosomal break repair: an emerging player in many games. Nat. Rev. Cancer 15, 137–151.

Bandyopadhyay, S., Mehta, M., Kuo, D., Sung, M.K., Chuang, R., Jaehnig, E.J., Bodenmiller, B., Licon, K., Copeland, W., Shales, M., et al. (2010).

Rewiring of genetic networks in response to DNA damage. Science 330, 1385–1389.

Bassik, M.C., Kampmann, M., Lebbink, R.J., Wang, S., Hein, M.Y., Poser, I., Weibezahn, J., Horlbeck, M.A., Chen, S., Mann, M., et al. (2013). A systematic mammalian genetic interaction map reveals pathways underlying ricin susceptibility. Cell 152, 909–922.

Basu, A., Bodycombe, N.E., Cheah, J.H., Price, E.V., Liu, K., Schaefer, G.I., Ebright, R.Y., Stewart, M.L., Ito, D., Wang, S., et al. (2013). An interactive resource to identify cancer genetic and lineage dependencies targeted by small molecules. Cell 154, 1151–1161.

Birmingham, A., Selfors, L.M., Forster, T., Wrobel, D., Kennedy, C.J., Shanks, E., Santoyo-Lopez, J., Dunican, D.J., Long, A., Kelleher, D., et al. (2009). Statistical methods for analysis of high-throughput RNA interference screens. Nat. Methods 6, 569–575.

Brody, L.C. (2005). Treating cancer by targeting a weakness. N. Engl. J. Med. 353, 949–950.

Cancer Genome Atlas Network (2012). Comprehensive molecular characterization of human colon and rectal cancer. Nature 487, 330–337.

Carrassa, L., Chilà, R., Lupi, M., Ricci, F., Celenza, C., Mazzoletti, M., Broggini, M., and Damia, G. (2012). Combined inhibition of Chk1 and Wee1: in vitro synergistic effect translates to tumor growth inhibition in vivo. Cell Cycle 11, 2507–2517.

Cerami, E., Gao, J., Dogrusoz, U., Gross, B.E., Sumer, S.O., Aksoy, B.A., Jacobsen, A., Byrne, C.J., Heuer, M.L., Larsson, E., et al. (2012). The cBio cancer genomics portal: an open platform for exploring multidimensional cancer genomics data. Cancer Discov. 2, 401–404.

Chan, D.A., and Giaccia, A.J. (2011). Harnessing synthetic lethal interactions in anticancer drug discovery. Nat. Rev. Drug Discov. 10, 351–364.

Chen, C.C., Kennedy, R.D., Sidi, S., Look, A.T., and D'Andrea, A. (2009). CHK1 inhibition as a strategy for targeting Fanconi Anemia (FA) DNA repair pathway deficient tumors. Mol. Cancer 8, 24.

Chilà, R., Basana, A., Lupi, M., Guffanti, F., Gaudio, E., Rinaldi, A., Cascione, L., Restelli, V., Tarantelli, C., Bertoni, F., et al. (2015). Combined inhibition of Chk1 and Wee1 as a new therapeutic strategy for mantle cell lymphoma. Oncotarget 6, 3394–3408.

Choueiri, M.B., Shen, J.P., Gross, A.M., Huang, J.K., Ideker, T., and Fanta, P. (2015). ERCC1 and TS Expression as Prognostic and Predictive Biomarkers in Metastatic Colon Cancer. PLoS ONE 10, e0126898.

Ciriello, G., Cerami, E., Sander, C., and Schultz, N. (2012). Mutual exclusivity analysis identifies oncogenic network modules. Genome Res. 22, 398–406.

Collette, L., and Tombal, B. (2015). N-of-1 trials in oncology. Lancet Oncol. 16, 885–886.

Collins, S.R., Schuldiner, M., Krogan, N.J., and Weissman, J.S. (2006). A strategy for extracting and analyzing large-scale quantitative epistatic interaction data. Genome Biol. 7, R63.

Collins, S.R., Miller, K.M., Maas, N.L., Roguev, A., Fillingham, J., Chu, C.S., Schuldiner, M., Gebbia, M., Recht, J., Shales, M., et al. (2007). Functional dissection of protein complexes involved in yeast chromosome biology using a genetic interaction map. Nature 446, 806–810.

Costanzo, M., Baryshnikova, A., Bellay, J., Kim, Y., Spear, E.D., Sevier, C.S., Ding, H., Koh, J.L., Toufighi, K., Mostafavi, S., et al. (2010). The genetic landscape of a cell. Science 327, 425–431.

Cowley, G.S., Weir, B.A., Vazquez, F., Tamayo, P., Scott, J.A., Rusin, S., East-Seletsky, A., Ali, L.D., Gerath, W.F., Pantel, S.E., et al. (2014). Parallel genome-scale loss of function screens in 216 cancer cell lines for the identification of context-specific genetic dependencies. Sci. Data 1, 140035.

Curtis, C., Shah, S.P., Chin, S.-F., Turashvili, G., Rueda, O.M., Dunning, M.J., Speed, D., Lynch, A.G., Samarajiwa, S., Yuan, Y., et al.; METABRIC Group (2012). The genomic and transcriptomic architecture of 2,000 breast tumours reveals novel subgroups. Nature 486, 346–352.

Deshpande, R., Asiedu, M.K., Klebig, M., Sutor, S., Kuzmin, E., Nelson, J., Piotrowski, J., Shin, S.H., Yoshida, M., Costanzo, M., et al. (2013). A

comparative genomic approach for identifying synthetic lethal interactions in human cancer. Cancer Res. *73*, 6128–6136.

Fabrizio, P., Hoon, S., Shamalnasab, M., Galbani, A., Wei, M., Giaever, G., Nislow, C., and Longo, V.D. (2010). Genome-wide screen in Saccharomyces cerevisiae identifies vacuolar protein sorting, autophagy, biosynthetic, and tRNA methylation genes involved in life span regulation. PLoS Genet. *6*, e1001024.

Fiedler, D., Braberg, H., Mehta, M., Chechik, G., Cagney, G., Mukherjee, P., Silva, A.C., Shales, M., Collins, S.R., van Wageningen, S., et al. (2009). Functional organization of the S. cerevisiae phosphorylation network. Cell *136*, 952–963.

Fong, P.C., Boss, D.S., Yap, T.A., Tutt, A., Wu, P., Mergui-Roelvink, M., Mortimer, P., Swaisland, H., Lau, A., O'Connor, M.J., et al. (2009). Inhibition of poly(ADP-ribose) polymerase in tumors from BRCA mutation carriers. N. Engl. J. Med. *361*, 123–134.

Griffith, M., Griffith, O.L., Coffman, A.C., Weible, J.V., McMichael, J.F., Spies, N.C., Koval, J., Das, I., Callaway, M.B., Eldred, J.M., et al. (2013). DGIdb: mining the druggable genome. Nat. Methods *10*, 1209–1210.

Guénolé, A., Srivas, R., Vreeken, K., Wang, Z.Z., Wang, S., Krogan, N.J., Ideker, T., and van Attikum, H. (2013). Dissection of DNA damage responses using multiconditional genetic interaction maps. Mol. Cell *49*, 346–358.

Hartwell, L.H., Szankasi, P., Roberts, C.J., Murray, A.W., and Friend, S.H. (1997). Integrating genetic approaches into the discovery of anticancer drugs. Science *278*, 1064–1068.

Hofree, M., Shen, J.P., Carter, H., Gross, A., and Ideker, T. (2013). Network-based stratification of tumor mutations. Nat. Methods *10*, 1108–1115.

Huang, M.E., Rio, A.G., Nicolas, A., and Kolodner, R.D. (2003). A genomewide screen in Saccharomyces cerevisiae for genes that suppress the accumulation of mutations. Proc. Natl. Acad. Sci. USA *100*, 11529–11534.

Jackson, A.L., and Linsley, P.S. (2010). Recognizing and avoiding siRNA off-target effects for target identification and therapeutic application. Nat. Rev. Drug Discov. *9*, 57–67.

Jerby-Arnon, L., Pfetzer, N., Waldman, Y.Y., McGarry, L., James, D., Shanks, E., Seashore-Ludlow, B., Weinstock, A., Geiger, T., Clemons, P.A., et al. (2014). Predicting cancer-specific vulnerability via data-driven detection of synthetic lethality. Cell *158*, 1199–1209.

Kaur, S., Modi, P., Srivastava, V., Mudgal, R., Tikoo, S., Arora, P., Mohanty, D., and Sengupta, S. (2010). Chk1-dependent constitutive phosphorylation of BLM helicase at serine 646 decreases after DNA damage. Mol. Cancer Res. *8*, 1234–1247.

Lord, C.J., Tutt, A.N., and Ashworth, A. (2015). Synthetic lethality and cancer therapy: lessons learned from the development of PARP inhibitors. Annu. Rev. Med. *66*, 455–470.

Martins, M.M., Zhou, A.Y., Corella, A., Horiuchi, D., Yau, C., Rakshandehroo, T., Gordan, J.D., Levin, R.S., Johnson, J., Jascur, J., et al. (2015). Linking tumor mutations to drug responses via a quantitative chemical-genetic interaction map. Cancer Discov. *5*, 154–167.

Morris, L.G., and Chan, T.A. (2015). Therapeutic targeting of tumor suppressor genes. Cancer *121*, 1357–1368.

Nei, M., Xu, P., and Glazko, G. (2001). Estimation of divergence times from multiprotein sequences for a few mammalian species and several distantly related organisms. Proc. Natl. Acad. Sci. USA *98*, 2497–2502.

Nijman, S.M., and Friend, S.H. (2013). Cancer. Potential of the synthetic lethality principle. Science *342*, 809–811.

Origanti, S., Cai, S.R., Munir, A.Z., White, L.S., and Piwnica-Worms, H. (2013). Synthetic lethality of Chk1 inhibition combined with p53 and/or p21 loss during a DNA damage response in normal and tumor cells. Oncogene *32*, 577–588.

Pratt, D., Chen, J., Welker, D., Rivas, R., Pillich, R., Rynkov, V., Ono, K., Miello, C., Hicks, L., Szalma, S., et al. (2015). NDEx, the Network Data Exchange. Cell Syst. *1*, 302–305.

Putnam, C.D., Allen-Soltero, S.R., Martinez, S.L., Chan, J.E., Hayes, T.K., and Kolodner, R.D. (2012). Bioinformatic identification of genes suppressing genome instability. Proc. Natl. Acad. Sci. USA *109*, E3251–E3259.

Roguev, A., Wiren, M., Weissman, J.S., and Krogan, N.J. (2007). High-throughput genetic interaction mapping in the fission yeast Schizosaccharomyces pombe. Nat. Methods *4*, 861–866.

Roguev, A., Bandyopadhyay, S., Zofall, M., Zhang, K., Fischer, T., Collins, S.R., Qu, H., Shales, M., Park, H.O., Hayles, J., et al. (2008). Conservation and rewiring of functional modules revealed by an epistasis map in fission yeast. Science *322*, 405–410.

Roguev, A., Talbot, D., Negri, G.L., Shales, M., Cagney, G., Bandyopadhyay, S., Panning, B., and Krogan, N.J. (2013). Quantitative genetic-interaction mapping in mammalian cells. Nat. Methods *10*, 432–437.

Russ, A.P., and Lampel, S. (2005). The druggable genome: an update. Drug Discov. Today *10*, 1607–1610.

Ryan, C.J., Roguev, A., Patrick, K., Xu, J., Jahari, H., Tong, Z., Beltrao, P., Shales, M., Qu, H., Collins, S.R., et al. (2012). Hierarchical modularity and the evolution of genetic interactomes across species. Mol. Cell *46*, 691–704.

Sawyers, C. (2004). Targeted cancer therapy. Nature *432*, 294–297.

Schittek, B., and Sinnberg, T. (2014). Biological functions of casein kinase 1 isoforms and putative roles in tumorigenesis. Mol. Cancer *13*, 231.

Schwaederle, M., Parker, B.A., Schwab, R.B., Fanta, P.T., Boles, S.G., Daniels, G.A., Bazhenova, L.A., Subramanian, R., Coutinho, A.C., Ojeda-Fournier, H., et al. (2014). Molecular tumor board: the University of California-San Diego Moores Cancer Center experience. Oncologist *19*, 631–636.

Shen, J.P., Srivas, R., Gross, A., Li, J., Jaehnig, E.J., Sun, S.M., Bojorquez-Gomez, A., Licon, K., Sivaganesh, V., Xu, J.L., et al. (2015). Chemogenetic profiling identifies RAD17 as synthetically lethal with checkpoint kinase inhibition. Oncotarget *6*, 35755–35769.

Simon, J.A., Szankasi, P., Nguyen, D.K., Ludlow, C., Dunstan, H.M., Roberts, C.J., Jensen, E.L., Hartwell, L.H., and Friend, S.H. (2000). Differential toxicities of anticancer agents among DNA repair and checkpoint mutants of Saccharomyces cerevisiae. Cancer Res. *60*, 328–333.

Srivas, R., Costelloe, T., Carvunis, A.R., Sarkar, S., Malta, E., Sun, S.M., Pool, M., Licon, K., van Welsem, T., van Leeuwen, F., et al. (2013). A UV-induced genetic network links the RSC complex to nucleotide excision repair and shows dose-dependent rewiring. Cell Rep. *5*, 1714–1724.

Tang, J.B., Svilar, D., Trivedi, R.N., Wang, X.H., Goellner, E.M., Moore, B., Hamilton, R.L., Banze, L.A., Brown, A.R., and Sobol, R.W. (2011). N-methylpurine DNA glycosylase and DNA polymerase beta modulate BER inhibitor potentiation of glioma cells to temozolomide. Neuro-oncol. *13*, 471–486.

Thompson, R., and Eastman, A. (2013). The cancer therapeutic potential of Chk1 inhibitors: how mechanistic studies impact on clinical trial design. Br. J. Clin. Pharmacol. *76*, 358–369.

Tong, A.H., and Boone, C. (2006). Synthetic genetic array analysis in Saccharomyces cerevisiae. Methods Mol. Biol. *313*, 171–192.

Tsai, S.Q., Zheng, Z., Nguyen, N.T., Liebers, M., Topkar, V.V., Thapar, V., Wyvekens, N., Khayter, C., Iafrate, A.J., Le, L.P., et al. (2015). GUIDE-seq enables genome-wide profiling of off-target cleavage by CRISPR-Cas nucleases. Nat. Biotechnol. *33*, 187–197.

van Pel, D.M., Barrett, I.J., Shimizu, Y., Sajesh, B.V., Guppy, B.J., Pfeifer, T., McManus, K.J., and Hieter, P. (2013). An evolutionarily conserved synthetic lethal interaction network identifies FEN1 as a broad-spectrum target for anti-cancer therapeutic development. PLoS Genet. *9*, e1003254.

Vance, J.R., and Wilson, T.E. (2002). Yeast Tdp1 and Rad1-Rad10 function as redundant pathways for repairing Top1 replicative damage. Proc. Natl. Acad. Sci. USA *99*, 13669–13674.

Cancer Genome Atlas Research Network, Weinstein, J.N., Collisson, E.A., Mills, G.B., Shaw, K.R.M., Ozenberger, B.A., Ellrott, K., Shmulevich, I.,

Sander, C., and Stuart, J.M. (2013). The cancer genome atlas pan-cancer analysis project. Nat. Genet. *45*, 1113–1120.

Wilmes, G.M., Bergkessel, M., Bandyopadhyay, S., Shales, M., Braberg, H., Cagney, G., Collins, S.R., Whitworth, G.B., Kress, T.L., Weissman, J.S., et al. (2008). A genetic interaction map of RNA-processing factors reveals links between Sem1/Dss1-containing complexes and mRNA export and splicing. Mol. Cell *32*, 735–746.

Wishart, D.S., Knox, C., Guo, A.C., Cheng, D., Shrivastava, S., Tzur, D., Gautam, B., and Hassanali, M. (2008). DrugBank: a knowledgebase for drugs, drug actions and drug targets. Nucleic Acids Res. *36*, D901–D906.

Wong, A.S., Choi, G.C., Cui, C.H., Pregernig, G., Milani, P., Adam, M., Perli, S.D., Kazer, S.W., Gaillard, A., Hermann, M., et al. (2016). Multiplexed barcoded CRISPR-Cas9 screening enabled by CombiGEM. Proc. Natl. Acad. Sci. USA *113*, 2544–2549.